Inorganic Chemistry

Article

pubs.acs.org/IC

Color Tuning and White Light Emission via in Situ Doping of Luminescent Lanthanide Metal–Organic Frameworks

Qun Tang,[†] Shuxia Liu,*[,†] Yiwei Liu,[†] Danfeng He,[†] Jun Miao,[†] Xingquan Wang,[†] Yujuan Ji,[†] and Zhiping Zheng*[,‡,§]

[†]Key Laboratory of Polyoxometalate Science of the Ministry of Education, College of Chemistry, Northeast Normal University, Changchun, Jilin 130024, China

[‡]Frontier Institute of Science and Technology, Xi'an Jiaotong University, Xi'an, Shaanxi 710054, China

[§]Department of Chemistry, University of Arizona, Tucson, Arizona 85721, United States

Supporting Information

ABSTRACT: Isostructural lanthanide metal–organic frameworks (MOFs) are synthesized through the spontaneous self-assembly of H_3BTPCA (1,1′,1″-(benzene-1,3,5-triyl)tripiperidine-4-carboxylic acid) ligands and lanthanide ions (we term these MOFs **Ln-BTPCA**, Ln = La^{3+}, Tb^{3+}, Sm^{3+}, etc.). Prompted by the observation that the different lanthanide ions have identical coordination environment in these MOFs, we explored and succeeded in the preparation of mixed-lanthanide analogues of the single-lanthanide MOFs by way of in situ doping using a mixture of lanthanide salts. With careful adjustment of the relative concentration of the lanthanide ions, the color of the luminescence can be modulated, and white light-emission can indeed be achieved. The mechanisms possibly responsible for the observed photophysical properties of these mixed-lanthanide MOFs are also discussed.

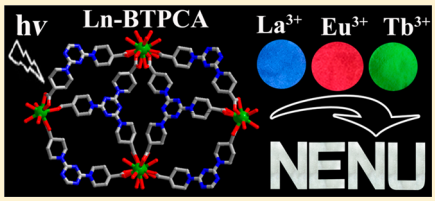

INTRODUCTION

Materials capable of producing high-intensity white light are important for applications in solid-state lighting and large-panel displays.[1] Obtaining such materials has been a considerable challenge. Single-component materials capable of white-light production are rare, and a more commonly adopted approach to achieving this goal has been to mix a blue or ultraviolet-emitting material with a yellow-emitting phosphor or to blend together materials that can emit in red, green, and blue, namely the three primary colors of light.[1a,2,3] Reported white-emitting materials include metal complexes,[4] metal-doped or hybrid inorganic materials,[5] small organic molecules,[6] quantum dots or nanocrystals,[7] and polymers.[8]

Light-emitting metal–organic frameworks (MOFs), that is, crystalline porous materials featuring metal atoms or complex units bridged by organic linking groups, represent a new class of light-emitting materials with the possibility of color tuning of the light emission, including the production of white light. As compared with the extensive studies aiming at the applications of such materials for gas separation/sorption[9] and catalysis,[10] the efforts in the design of luminescent MOFs are limited, although there have been a number of reports dealing with the production of luminescent MOFs and the tuning of the luminescence properties of these materials.[11,12]

Most notable among the reported luminescent MOFs are those that contain lanthanide elements. These include MOFs featuring lanthanide ions as an integral building component of the framework and those doped with lanthanide ions with no disruption of the original framework structure.[12−15] With the use of different lanthanide ions and the judicious choice of the bridging ligands, the luminescence properties of the resulting MOFs may be modulated. Adding more interest to such materials is the possibility of perturbing the lanthanide coordination with small guest molecules, frequently exchangeable coordinating solvent molecules, or the doping of other metal ions if the ligands are equipped with functional moieties capable of secondary metal complexation (with respect to the primary coordination of the lanthanide ions). Recently we reported a series of isostructural Ln-MOFs (Ln = Ce^{3+}, Pr^{3+}, Nd^{3+}, Eu^{3+}) of the general formula $[Ln(BTPCA)H_2O]\cdot 2DMF\cdot 3H_2O$ where the ligand BTPCA is 1,1′,1″-(benzene-1,3,5-triyl)tripiperidine-4-carboxylate.[16] Isostructural analogues with the use of La^{3+}, Sm^{3+}, and Tb^{3+}, reported for the first time in this work, have also been synthesized. For the Eu^{3+}-containing MOF, the interactions of various transition metal ions with the free triazinyl N atoms were shown to affect the intensity of the characteristic red emission, based on which sensing of specific metal ions may be achieved.

Of particular interest to the fine-tuning of light-emitting properties of these MOF materials is the identical coordination environment of the different lanthanide ions. The similarity in chemical reactivity and coordination behavior of different lanthanide ions suggests that isostructural MOFs with mixed lanthanide ions may be achieved via in situ doping, and most significantly, depending on the types and relative concentration of the constituent lanthanide ions, the color of the light emission may be modulated. Ultimately, white-light-emitting

Received: September 2, 2013
Published: December 13, 2013

materials may be realized if the mixing of the metal ions can be carefully controlled. Fundamentally, such an isostructural system, not generally available, provides a perfect platform for detailed investigation of the energy transfer between the ligand and the lanthanide ions and the transfer between different metal ions.

In this work, we report the preparation of the aforementioned three new MOFs, $[Ln(BTPCA)H_2O]\cdot 2DMF\cdot 3H_2O$ (we term these MOFs **Ln-BTPCA**, Ln = La^{3+}, Sm^{3+}, and Tb^{3+}) and a series of mixed lanthanide analogues. With careful adjustment of the relative concentration of the lanthanide ions, the color of the luminescence can be modulated, and white light-emission can indeed be achieved. The mechanisms possibly responsible for the observed photophysical properties of these mixed-lanthanide MOFs are also discussed.

EXPERIMENTAL SECTION

Materials and Methods. Lanthanide halide ($LnCl_3\cdot 6H_2O$, Ln = La^{3+}, Eu^{3+}, Tb^{3+}, Sm^{3+}, Ce^{3+}, Pr^{3+}, and Nd^{3+}) and solvents used were purchased and used without further purification. H_3BTPCA was synthesized by following a literature report and characterized by infrared (IR) spectroscopy and single-crystal X-ray diffraction.[17] The IR spectra (KBr pellets) were recorded in the range 400−4000 cm^{-1} with an Alpha Centauri FT/IR spectrophotometer (Figure S1 in the Supporting Information). Elemental analyses (C, N, and H) were performed on a Perkin−Elmer 2400 CHN elemental analyzer. Elemental analyses for La, Eu, and Tb were obtained using a PLASMA-SPEC(I) ICP atomic emission spectrometer. Thermogravimetric analyses were carried out with a PerkinElmer TGA7 instrument, with a heating rate of 10 °C/min and under a nitrogen atmosphere (Figure S2, Supporting Information). Powder X-ray diffraction (XRD) measurements were performed with a Rigaku D/MAX-3 instrument with Cu Kα radiation in the 2θ range of 3−60° at 293 K. Photoluminescence spectra were obtained by using a FLSP 920 Edinburgh instrument (Eng) with 450 W xenon lamp monochromatized by double grating. The luminescence decay curves were obtained at room temperature on Edinburgh Instruments FLSP 920 based on time correlated photon counting. The quantum yield measurements were carried out on solid samples using an integrating sphere mounted on the FLSP 920 Edinburgh instrument. The Commission International de l'Eclairage (CIE) color coordinates were calculated by following the international CIE standards.[18]

Synthesis of [Ln(BTPCA)] Materials. All compounds including the mixed-lanthanide ones were obtained by adopting an otherwise identical procedure except for the different starting lanthanide salts. The synthesis of $[La(BTPCA)H_2O]\cdot 2DMF\cdot 3H_2O$ (**La-BTPCA**) is thus presented here in detail as a representative: A mixture containing $LaCl_3\cdot 6H_2O$ (71 mg, 0.20 mmol), H_3BTPCA (93 mg, 0.2 mmol), dimethylformamide (DMF, 10 mL), and H_2O (10 mL) was stirred at room temperature for 1 h and then at 65 °C (oil bath) for 72 h. The product was isolated as colorless needle-like crystals upon cooling of the reaction mixture, collected by filtration, washed with DMF and deionized water, and dried under vacuum (yield 0.118 g, 72% based on La). Anal. Calcd for $C_{27}H_{49}LaN_8O_{12}$ (%): C, 39.71; H, 6.05; N, 13.72. Found: C, 39.88; H, 6.12; N, 13.35. IR (KBr pallet, cm^{-1}): 3425(s), 2933(s), 2846(s), 1675(s), 1540(s), 1425(m), 1226(s), 1091(s), 1020(s), 933(s), 782(s), 504(s). Anal. Calcd for $[Tb(BTPCA)H_2O]\cdot 2DMF\cdot 3H_2O$ (**Tb-BTPCA**): C, 38.76; H, 5.90; N, 13.39;. Found: C, 38.98; H, 6.01; N, 13.04. Anal. Calcd for $[Sm(BTPCA)H_2O]\cdot 2DMF\cdot 3H_2O$ (**Sm-BTPCA**): C, 39.16; H, 5.96; N, 13.53. Found: C, 39.43; H, 5.85; N, 13.27.

Compounds containing mixed lanthanide ions, including **La_xEu_{1-x}-BTPCA**, **La_yTb_{1-y}-BTPCA**, **Eu_zTb_{1-z}-BTPCA**, and **$La_xEu_yTb_{1-x-y}$-BTPCA**, were prepared by using a mixture containing the desired lanthanide halides. Analyses of the relative molar concentration of the individual lanthanide elements are consistent with the corresponding ratios in the starting mixture (Table S1 and S2 in the Supporting Information).

Single Crystal X-ray Diffraction Data Collections and Structure Determination. Single-crystal diffraction data were collected at room temperature using a Bruker Smart Apex CCD diffractometer with Mo Kα monochromated radiation (λ = 0.71073 Å). The linear absorption coefficients, scattering factors for the atoms, and anomalous dispersion corrections were taken from the International Tables for X-ray Crystallography.[19] Empirical absorption corrections were applied. The structures were solved by using the direct method and refined through the full matrix least-squares method on F^2 using SHELXS-97.[20] Anisotropic thermal parameters were used to refine all non-hydrogen atoms, with the exception of some oxygen atoms. Those hydrogen atoms attached to the lattice water molecules were not located. Isolated solvent molecules within the channels were not crystallographically well-defined. The number of water and DMF molecules of crystallization were estimated by thermogravimetry, and only a fraction of the oxygen atoms were determined with the crystallographic analysis. The detailed crystal information is presented in Table S3, Supporting Information. Further details of the structural analyses may be obtained from the Fachinformationszentrum Karlsruhe, 76344 Eggenstein-Leopoldshafen, Germany (fax: (+49)-7247-808-666; e-mail: crysdata@fiz-karlsruhe.de), on quoting the depository numbers: CCDC 954858, 879894, and 954859.

RESULTS AND DISCUSSION

Syntheses and Structures of Compounds. The isostructural Ln-MOFs including the mixed-lanthanide species were readily synthesized under mild conditions using lanthanide halide and the tricarboxylate ligand in a mixed solvent of DMF and water. The air-stable crystalline products are insoluble in water or any common organic solvents. The structures of the three single-lanthanide MOFs **Ln-BTPCA** (Ln = La^{3+}, Sm^{3+}, and Tb^{3+}) were determined crystallographically. These compounds are isostructural to the **Eu-BTPCA** whose structure has been described in detail in our recent report (Figure S3, Supporting Information). All of Ln(III) have the same coordination environment surrounded by eight O atoms from six different BTPCA ligands and one water molecule (Figure 1). That the powder X-ray diffraction patterns of these compounds (Figure S4−S6, Supporting Information) agree well with the simulated ones based on the corresponding single-crystal structural analysis further indicates the purity of the bulk crystalline products. For the mixed-lanthanide MOFs,

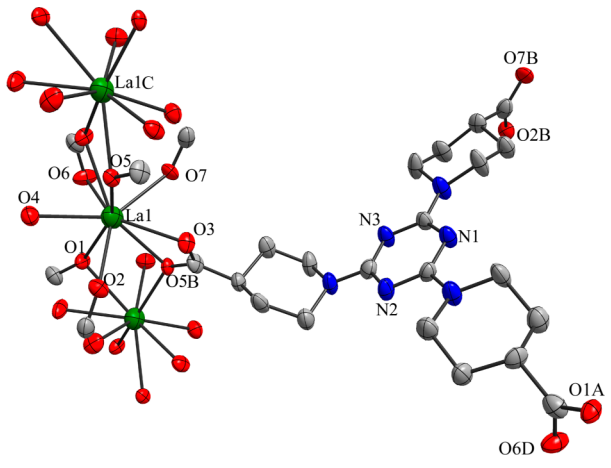

Figure 1. Representation of the La(III) coordination environments of compound **La-BTPCA**. Symmetry operation: A, 1 + x, 0.5 − y, 0.5 + z; B, 2 − x, 0.5 + y, 0.5 − z; C, x, 0.5 − y, 0.5 + z; D, 1 + x, y, z. All carbon H atoms and lattice solvent molecules are omitted for clarity. Displacement ellipsoids are drawn at the 50% probability level.

dx.doi.org/10.1021/ic402228g | Inorg. Chem. 2014, 53, 289−293

the molar ratio of the lanthanide elements is essentially the same as in the corresponding starting mixture, clearly suggesting that in situ doping of the lanthanide ions was successful. As can be seen from the cell parameters of their single crystals (Table S4, Supporting Information) and their powder XRD patterns (Figure S7, Supporting Information), the mixed lanthanide MOFs are also isostructural to their single-lanthanide analogues.

Photoluminescence Properties. The luminescence properties of Ln-MOFs are of interest for solid-state lighting applications. These materials are even more intriguing when the ligand used is also capable of light emission when excited. In the present case, upon excitation at 365 nm, powder samples of single-lanthanide MOFs **Ln-BTPCA** (Ln = Eu^{3+}, Tb^{3+}, and La^{3+}) emit red, green, and blue light, respectively (Figure 2).

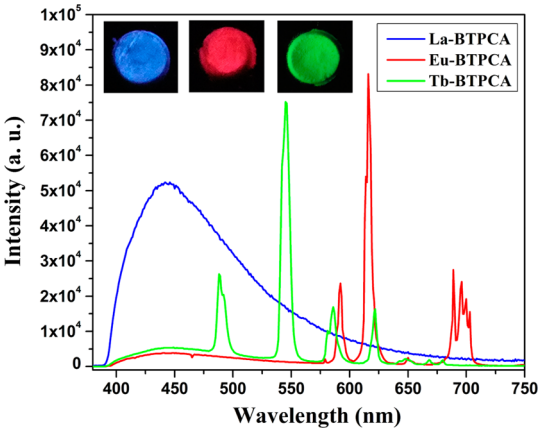

Figure 2. Emission spectra of complexes **La-BTPCA**, **Eu-BTPCA**, and **Tb-BTPCA** in the solid state at room temperature (λ_{ex} = 365 nm).

The excitation spectrum of **La-BTPCA** consists of a broad band with a maximum at about 365 nm, which can be ascribed to the $\pi-\pi^*$ electronic transition of the BTPCA ligand (Figure S8, Supporting Information). The emission spectrum of **La-BTPCA** shows a major peak at 445 nm, assignable to the ligand-to-metal energy transfer (Figure S9, Supporting Information). With respect to the emission of the pure ligand, the enhancement of intensity and the small red shift of the emission of **La-BTPCA** may be attributable to the increase of rigidity of the ligand upon coordination with the metal ion; increase of ligand rigidity helps reduce the loss of energy otherwise occurring via radiationless decay of the intraligand emission excited state.[21] The red and green emission of **Eu-BTPCA** and **Tb-BTPCA** are characteristic of Eu^{3+} and Tb^{3+} ions, respectively. In both cases, the ligand-based emission of 445 nm was not observed; thus, the ligand serving as an effective antenna for the excitation of the complexes and subsequent energy transfer to the emissive lanthanide ions is clearly established.

With the in situ doping of different lanthanide ions, the color of emission can be tuned. Ultimately, production of white light should be achievable if the right combination of different lanthanide ions in carefully adjusted molar ratio is incorporated into one MOF structure. Indeed, Eu^{3+} was doped into a host of **Tb-BTPCA** to afford $\mathbf{Eu_zTb_{1-z}}$**-BTPCA**, a mixed-lanthanide MOF. With the increase of the doped Eu^{3+} and upon excitation at 365 nm, the emission of this material shifted from the pure green emission of **Tb-BTPCA** to essentially pure red when z = 10%, as would be observed in **Eu-BTPCA**. The observation may be attributable to the enhanced probability of energy transfer from the Tb^{3+} to Eu^{3+} ions with the increase of Eu^{3+} ion concentration.[22] The emission spectra at various concentrations of doped Eu^{3+} in $\mathbf{Eu_zTb_{1-z}}$**-BTPCA** are shown in Figure 3. The gradual color change of the emission experimentally observed is consistent with calculated results (Figure S10, Supporting Information).

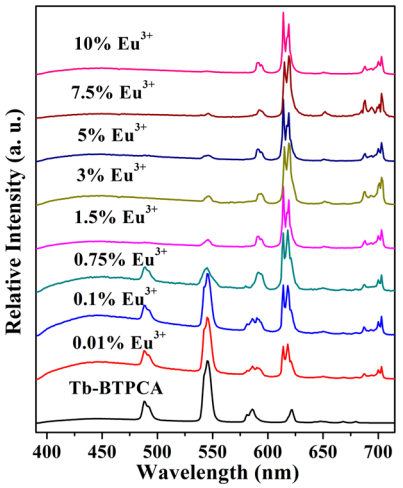

Figure 3. Emission spectra of the $\mathbf{Eu_zTb_{1-z}}$**-BTPCA** (z = 0−10 mol %) solid samples under 365 nm excitation.

The energy transfer behavior can be confirmed by the fluorescence dynamics of $\mathbf{Eu_zTb_{1-z}}$**-BTPCA**. The decay curves (Figure S11 and S12, Supporting Information) for the undoped **Tb-BTPCA** (monitored by $^5D_4 \rightarrow {}^7F_5$, 545 nm) and **Eu-BTPCA** (monitored by $^5D_0 \rightarrow {}^7F_2$, 618 nm) can be well fitted into a single exponential function as $I(t) = I_0 \exp(-t/\tau)$ (where τ is the 1/e lifetime of Tb^{3+} or Eu^{3+}). The lifetimes of **Tb-BTPCA** and **Eu-BTPCA** are 1.333 and 0.932 ms, respectively. We also investigated the fluorescence decay of the $^5D_4 \rightarrow {}^7F_5$ transition of the Tb^{3+} ion and the $^5D_0 \rightarrow {}^7F_2$ transition of Eu^{3+} ion in samples of $\mathbf{Eu_zTb_{1-z}}$**-BTPCA** (z = 0.1−10 mol %). It is clear that the concentration of doped Eu^{3+} profoundly modifies the fluorescent dynamics of the Tb^{3+} ion. The obtained effective lifetime of Tb^{3+} shortened, while that of Eu^{3+} increased with the increase of Eu^{3+} doping (Table 1; Figures S13 and S14, Supporting Information). These observations collectively point to the occurrence of energy transfer from Tb^{3+} to Eu^{3+} in $\mathbf{Eu_zTb_{1-z}}$**-BTPCA**. Observations of analogous energy transfer were reported for materials that contain both Tb^{3+} and Eu^{3+}.[14,22]

In order to achieve the production of white light emission, a more careful control of the amount of Eu^{3+} dopant is necessary. We found that the major peak of emission of Tb^{3+} at 545 nm is more intense than that of Eu^{3+} at 618 nm in $\mathbf{Eu_{0.0001}Tb_{0.9999}}$**-BTPCA**. In comparison, the relative intensity of these two emission peaks is reversed in $\mathbf{Eu_{0.0075}Tb_{0.9925}}$**-BTPCA**. Since white light emission can be produced when the emission intensities at 450, 545, and 618 nm are comparable, we made an effort to optimize the relative concentration of Tb^{3+} and Eu^{3+} in $\mathbf{Eu_zTb_{1-z}}$**-BTPCA** while leaving the production of the blue emission at 450 nm to the inherently fixed amount of the BTPCA ligand in the framework structure. It has been found that with 99.5 mol % of Tb^{3+} and 0.5 mol % Eu^{3+} (the quantum yield is 46.15%), nearly pure white light emission was achieved with its CIE coordinate of (0.3264, 0.3308) being very close to

dx.doi.org/10.1021/ic402228g | Inorg. Chem. 2014, 53, 289−293

Table 1. The Lifetime for Tb^{3+} and Eu^{3+} Ions in the Eu_zTb_{1-z}-BTPCA Monitored by the $^5D_4 \rightarrow {}^7F_5$ Transition at 545 nm and the $^5D_0 \rightarrow {}^7F_2$ Transition at 618 nm (λ_{ex} = 365 nm)

	z									
	0	0.01%	0.1%	0.75%	1.5%	3%	5%	7.5%	10%	100%
$\tau_{Tb^{3+}}$, ms	1.333	1.277	1.204	0.435	0.232	0.145	0.113	0.097	0.002	0
$\tau_{Eu^{3+}}$, ms	0	0.570	0.585	0.616	0.668	0.681	0.733	0.798	0.856	0.932

the coordinate for pure white-light (0.3333, 0.3333) (Figure 4). The correlated color temperatures (CCT) are 5818, 9569, and

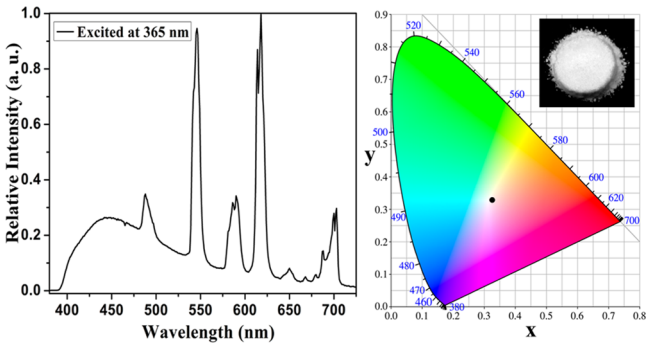

Figure 4. Emission spectra of **$Eu_{0.005}Tb_{0.995}$-BTPCA** with excitation at 365 nm (left) and the CIE chromaticity diagram for **$Eu_{0.005}Tb_{0.995}$-BTPCA** monitored with the excitation at 365 nm (right). Inset: optical photograph of a powder sample of **$Eu_{0.005}Tb_{0.995}$-BTPCA** excited using a UV lamp at 365 nm.

6572 K for **$Eu_{0.005}Tb_{0.995}$-BTPCA**, **$Eu_{0.001}Tb_{0.999}$-BTPCA**, and **$Eu_{0.0075}Tb_{0.9925}$-BTPCA**, respectively. The lifetime of the broad band emission was measured by exciting the powder sample with a laser at 365 nm. The decay curves were single exponential with lifetimes of 1.072 ms (monitored at 545 nm) and 0.592 ms (monitored at 618 nm) (Figure S15, Supporting Information). From these results, it is clear that the blue emission of the BTPCA ligand, the green emission of Tb^{3+}, and the red emission of Eu^{3+} occur simultaneously, producing the white light emission.

Considering that **La-BTPCA** emits in blue, one may anticipate the production of white light emission if the parent **La-BTPCA** can be codoped with both Tb^{3+} and Eu^{3+}. Indeed, upon excitation at 365 nm, samples of **$La_xEu_yTb_{1-x-y}$-BTPCA** display a wide spectrum of emission in the visible range with varying relative intensity of emission at 612 (Eu^{3+}), 545 (Tb^{3+}) and 450 (the ligand) nm depending on the concentration of the Tb^{3+}/Eu^{3+} dopants (Figure 5). The optimal concentrations of the codopants for white light emission are 10 mol % Eu^{3+}, 30 mol % Tb^{3+} (the quantum yield is 47.33%, $\tau_{Tb^{3+}}$ = 1.027 ms, $\tau_{Eu^{3+}}$ = 0.594 ms) (Figure S16, Supporting Information) with the corresponding CIE coordinate (0.3161, 0.3212). The CCT value of **$La_{0.6}Eu_{0.1}Tb_{0.3}$-BTPCA** is 6370 K. The CIE chromaticity coordinates for the other species of **$La_xEu_yTb_{1-x-y}$-BTPCA** with various ratios of La/Tb/Eu are collected in Table S5, Supporting Information.

The emission spectra of the monodoped **La_xEu_{1-x}-BTPCA** and **La_yTb_{1-y}-BTPCA** were also investigated, both exhibiting emissions characteristic of Eu^{3+}, Tb^{3+}, or ligand-to-metal charge transfer (Figure S17 and S18, Supporting Information). It is of note that the Eu^{3+}- or Tb^{3+}-based emissions are systematically more intense than that of the BTPCA ligand, suggesting partial energy transfer from La^{3+} to Eu^{3+} or Tb^{3+} ions and that the Ln^{3+}-centered luminescence is significantly sensitized by the

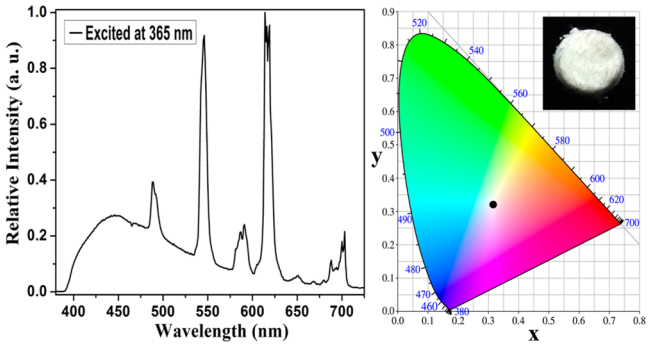

Figure 5. Emission spectra of **$La_{0.6}Eu_{0.1}Tb_{0.3}$-BTPCA** excitation at 365 nm (left). The CIE chromaticity diagram for **$La_{0.6}Eu_{0.1}Tb_{0.3}$-BTPCA** monitored under 365 nm (right). The inset is the optical photograph excited under 365 nm UV lamps.

semirigid ligand. The corresponding photographs of the tunable colors generated from **La_xEu_{1-x}-BTPCA** and **La_yTb_{1-y}-BTPCA** when excited with a UV lamp at 365 nm are shown in Figures S19 and S20, Supporting Information. With the increase of doped Eu^{3+} or Tb^{3+}, color-tuning of the emission can be achieved from blue to blue-red and blue-green.

CONCLUSIONS

In summary, we have developed a simple and facile one-step approach for the synthesis of lanthanide metal−organic frameworks. The identical coordination behavior of the different lanthanide ions allows in situ doping of various lanthanide ions into a parent MOF, and the color of luminescence of the resulting isostructural materials can be fine-tuned and optimized for the ultimate production of white light emission. The preparation of nanostructured materials of these crystalline MOFs and the fabrication of light-emitting devices using these materials as phosphors are in progress.

ASSOCIATED CONTENT

Supporting Information

X-ray crystallographic data for **La-BTPCA**, **Tb-BTPCA**, and **Sm-BTPCA** in CIF format, X-ray crystallographic data and structural refinement, packing diagram, elemental analyses data, IR spectra, TGA analyses, powder XRD patterns, excitation and emission spectra, decay curves, and CIE chromaticity coordinates diagram for **Ln-BTPCA**. This material is available free of charge via the Internet at http://pubs.acs.org.

AUTHOR INFORMATION

Corresponding Authors

*E-mail: liusx@nenu.edu.cn (S. L.).
*E-mail: zhiping@email.arizona.edu (Z. Z.).

Notes

The authors declare no competing financial interest.

dx.doi.org/10.1021/ic402228g | Inorg. Chem. 2014, 53, 289−293

■ ACKNOWLEDGMENTS

This work was supported by the NSFC (Grants 21171032 and 21231002), Fundamental Research Funds for the Central Universities (Grant 09ZDQD0015), and the Open Research Fund of the State Key Laboratory of Inorganic Synthesis and Preparative Chemistry (Jilin University, Grant 2012-10).

■ REFERENCES

(1) (a) Schubert, E. F.; Kim, J. K. *Science* **2005**, *308*, 1274. (b) Feldmann, C.; Jüstel, T.; Ronda, C. R.; Schmidt, P. J. *Adv. Funct. Mater.* **2003**, *13*, 511.

(2) (a) Zhu, X.-H.; Peng, J.; Cao, Y.; Roncali, J. *Chem. Soc. Rev.* **2011**, *40*, 3509. (b) Mao, Z.-y.; Wang, D.-j. *Inorg. Chem.* **2010**, *49*, 4922. (c) Huang, C.-H.; Chen, T.-M. *Inorg. Chem.* **2011**, *50*, 5725.

(3) (a) Sasabe, H.; Kido, J. *Chem. Mater.* **2010**, *23*, 621. (b) Liu, J.; Yang, Q.; Zhang, L.; Jiang, D.; Shi, X.; Yang, J.; Zhong, H.; Li, C. *Adv. Funct. Mater.* **2007**, *17*, 569.

(4) (a) Coppo, P.; Duati, M.; Kozhevnikov, V. N.; Hofstraat, J. W.; De Cola, L. *Angew. Chem., Int. Ed.* **2005**, *44*, 1806. (b) Jayaramulu, K.; Kanoo, P.; George, S. J.; Maji, T. K. *Chem. Commun.* **2010**, *46*, 79068. (c) Wibowo, A. C.; Vaughn, S. A.; Smith, M. D.; zur Loye, H.-C. *Inorg. Chem.* **2010**, *49*, 11001. (d) Xu, H.-B.; Chen, X.-M.; Zhang, Q.-S.; Zhang, L.-Y.; Chen, Z.-N. *Chem. Commun.* **2009**, 7318.

(5) (a) Roushan, M.; Zhang, X.; Li, J. *Angew. Chem., Int. Ed.* **2012**, *51*, 436. (b) Green, W. H.; Le, K. P.; Grey, J.; Au, T. T.; Sailor, M. J. *Science* **1997**, *276*, 1826. (c) Liao, Y.-C.; Lin, C.-H.; Wang, S.-L. *J. Am. Chem. Soc.* **2005**, *127*, 9986. (d) Lima, P. c. P.; Almeida Paz, F. A.; Ferreira, R. A. S.; de Zea Bermudez, V.; Carlos, L. S. D. *Chem. Mater.* **2009**, *21*, 5099. (e) Luo, L.; Zhang, X. X.; Li, K. F.; Cheah, K. W.; Shi, J. X.; Wong, W. K.; Gong, M. L. *Adv. Mater.* **2004**, *16*, 1664.

(6) (a) Zhao, Y. S.; Fu, H. B.; Hu, F. Q.; Peng, A. D.; Yang, W. S.; Yao, J. N. *Adv. Mater.* **2008**, *20*, 79. (b) Mazzeo, M.; Vitale, V.; Della Sala, F.; Anni, M.; Barbarella, G.; Favaretto, L.; Sotgiu, G.; Cingolani, R.; Gigli, G. *Adv. Mater.* **2005**, *17*, 34.

(7) (a) Ju, Q.; Tu, D.; Liu, Y.; Li, R.; Zhu, H.; Chen, J.; Chen, Z.; Huang, M.; Chen, X. *J. Am. Chem. Soc.* **2012**, *134*, 1323. (b) Sun, Z.; Bai, F.; Wu, H.; Boye, D. M.; Fan, H. *Chem. Mater.* **2012**, *24*, 3415. (c) Bowers, M. J.; McBride, J. R.; Rosenthal, S. J. *J. Am. Chem. Soc.* **2005**, *127*, 15378.

(8) He, G.; Guo, D.; He, C.; Zhang, X.; Zhao, X.; Duan, C. *Angew. Chem., Int. Ed.* **2009**, *48*, 6132.

(9) (a) Li, J.-R.; Sculley, J.; Zhou, H.-C. *Chem. Rev.* **2011**, *112*, 869. (b) Suh, M. P.; Park, H. J.; Prasad, T. K.; Lim, D.-W. *Chem. Rev.* **2011**, *112*, 782. (c) Murray, L. J.; Dinca, M.; Long, J. R. *Chem. Soc. Rev.* **2009**, *3*, 1294. (d) Li, J.-R.; Kuppler, R. J.; Zhou, H.-C. *Chem. Soc. Rev.* **2009**, *38*, 1477.

(10) (a) Yoon, M.; Srirambalaji, R.; Kim, K. *Chem. Rev.* **2011**, *112*, 1196. (b) Ma, L.; Abney, C.; Lin, W. *Chem. Soc. Rev.* **2009**, *3*, 1248. (c) Lee, J.; Farha, O. K.; Roberts, J.; Scheidt, K. A.; Nguyen, S. T.; Hupp, J. T. *Chem. Soc. Rev.* **2009**, *38*, 1450.

(11) (a) Kreno, L. E.; Leong, K.; Farha, O. K.; Allendorf, M.; Van Duyne, R. P.; Hupp, J. T. *Chem. Rev.* **2011**, *112*, 1105. (b) Rocha, J.; Carlos, L. D.; Paz, F. A.; Ananias, D. *Chem. Soc. Rev.* **2011**, *40*, 926. (c) Bünzli, J.-C. G. *Chem. Rev.* **2010**, *110*, 2729. (d) Allendorf, M. D.; Bauer, C. A.; Bhakta, R. K.; Houk, R. J. T. *Chem. Soc. Rev.* **2009**, *38*, 1330.

(12) (a) Cui, Y.; Yue, Y.; Qian, G.; Chen, B. *Chem. Rev.* **2012**, *112*, 1126. (b) Falcaro, P.; Furukawa, S. *Angew. Chem., Int. Ed.* **2012**, *51*, 8431. (c) de Lill, D. T.; de Bettencourt-Dias, A.; Cahill, C. L. *Inorg. Chem.* **2007**, *46*, 3960.

(13) (a) Rao, X.; Huang, Q.; Yang, X.; Cui, Y.; Yang, Y.; Wu, C.; Chen, B.; Qian, G. *J. Mater. Chem.* **2012**, *22*, 3210. (b) Dang, S.; Zhang, J.-H.; Sun, Z.-M. *J. Mater. Chem.* **2012**, *22*, 8868. (c) Li, S. M.; Zheng, X. J.; Yuan, D. Q.; Ablet, A.; Jin, L. P. *Inorg. Chem.* **2012**, *51*, 1201. (d) Sava, D. F.; Rohwer, L. E.; Rodriguez, M. A.; Nenoff, T. M. *J. Am. Chem. Soc.* **2012**, *134*, 3983. (e) Ma, X.; Li, X.; Cha, Y.-E.; Jin, L.-P. *Cryst. Growth Des.* **2012**, *12*, 5227. (f) Luo, Y.; Calvez, G.; Freslon, S.; Bernot, K.; Daiguebonne, C.; Guillou, O. *Eur. J. Inorg. Chem.* **2011**, *2011*, 3705.

(14) (a) Zhong, S.-L.; Xu, R.; Zhang, L.-F.; Qu, W.-G.; Gao, G.-Q.; Wu, X.-L.; Xu, A.-W. *J. Mater. Chem.* **2011**, *21*, 16574. (b) Liu, K.; You, H.; Zheng, Y.; Jia, G.; Huang, Y.; Yang, M.; Song, Y.; Zhang, L.; Zhang, H. *Cryst. Growth Des.* **2010**, *10*, 16. (c) Guo, H.; Zhu, Y.; Qiu, S.; Lercher, J. A.; Zhang, H. *Adv. Mater.* **2010**, *22*, 4190. (d) Liu, K.; You, H.; Zheng, Y.; Jia, G.; Song, Y.; Huang, Y.; Yang, M.; Jia, J.; Guo, N.; Zhang, H. *J. Mater. Chem.* **2010**, *20*, 3272. (e) Amghouz, Z.; Garcia-Granda, S.; Garcia, J. R.; Ferreira, R. A.; Mafra, L.; Carlos, L. D.; Rocha, J. *Inorg. Chem.* **2012**, *51*, 1703. (f) Ma, M.-L.; Ji, C.; Zang, S.-Q. *Dalton Trans.* **2013**, *42*, 10579.

(15) (a) Rao, X.; Song, T.; Gao, J.; Cui, Y.; Yang, Y.; Wu, C.; Chen, B.; Qian, G. *J. Am. Chem. Soc.* **2013**, *135*, 15559. (b) Cadiau, A.; Brites, C. D. S.; Costa, P. M. F. J.; Ferreira, R. A. S.; Rocha, J.; Carlos, L. D. *ACS Nano* **2013**, *7*, 7213. (c) Cui, Y.; Xu, H.; Yue, Y.; Guo, Z.; Yu, J.; Chen, Z.; Gao, J.; Yang, Y.; Qian, G.; Chen, B. *J. Am. Chem. Soc.* **2012**, *134*, 3979. (d) Liu, T.-F.; Zhang, W.; Sun, W.-H.; Cao, R. *Inorg. Chem.* **2011**, *50*, 5242. (e) Jiang, Y.-Y.; Ren, S.-K.; Ma, J.-P.; Liu, Q.-K.; Dong, Y.-B. *Chem.—Eur. J.* **2009**, *15*, 10742. (f) Wang, P.; Ma, J.-P.; Dong, Y.-B.; Huang, R.-Q. *J. Am. Chem. Soc.* **2007**, *129*, 10620.

(16) Tang, Q.; Liu, S.; Liu, Y.; Miao, J.; Li, S.; Zhang, L.; Shi, Z.; Zheng, Z. *Inorg. Chem.* **2013**, *52*, 2799.

(17) Zhao, X. L.; He, H. Y.; Hu, T. P.; Dai, F. N.; Sun, D. F. *Inorg. Chem.* **2009**, *48*, 8057.

(18) Smith, T.; Guild, J. *Trans. Opt. Soc., London* **1931**, *33*, 73.

(19) *International Tables for X-ray Crystallography*; Henry, N. F. M.; Lonsdale, K., Eds.; Kynoch Press: Birmingham, U.K., 1952.

(20) Sheldrick, G. M. *SHELXS-97: Programs for Crystal Structure Solution*, University of Götingen: Götingen (Germany), 1997.

(21) Robin, A. Y.; Fromm, K. M. *Coord. Chem. Rev.* **2006**, *250*, 2127.

(22) Thompson, M. K.; Vuchkov, M.; Kahwa, I. A. *Inorg. Chem.* **2001**, *40*, 4332.